Journal of Shahrekord University of Medical Sciences
doi:10.34172/jsums.2021.06 2021;23(1):34-43 http://j.skums.ac.ir
Archive of SID

Original Article

Photocatalytic removal of naphthalene ($C_{10}H_8$) from aqueous environments using sulfur and nitrogen doped titanium dioxide (TiO_2-N-S) coated on glass microbullets in presence of sunlight

Abbas Jafari[1], Mehrban Sadeghi[1,2*], Farhang Tirgir[1,3], Mehdi Barghaei[4]

[1]PhD Candidate in Environmental Engineering, Faculty of Natural Resources and Environment, Islamic Azad University, Tehran Science and Research Branch, Tehran, Iran
[2]Professor of Environmental Health Engineering, Faculty of Public Health, Shahrekord University of Medical Sciences, Shahrekord, Iran
[3]Assistant Professor, Department of Chemistry, Faculty of Basic Sciences, Shahrekord Branch, Islamic Azad University, Shahrekord, Iran
[4]Professor of Environmental Engineering, Department of Chemistry and Environment, Technical and Engineering Faculty, Sharif University of Technology, Tehran, Iran

*Corresponding Author: Mehrban Sadeghi, Department of Environmental Health Engineering, School of Health, Shahrekord University of Medical Sciences, Shahrekord, Iran. Tel: +989133082426, Email: sadeghi@skums.ac.ir

Abstract

Background and aims: Due to their toxicity and carcinogenic effects, polycyclic aromatic hydrocarbons (PAHs) such as naphthalene ($C_{10}H_8$) are regarded as hazardous compounds for both humans and the environment, and it is essential to remove these contaminants from the environment. The present study aimed to remove naphthalene from a synthetic aqueous environment using sulfur and nitrogen doped titanium dioxide (TiO_2-N-S) nanoparticles (NPs) immobilized on glass microbullets under sunlight.

Methods: In this experimental study, TiO_2-N-S NPs were synthesized using sol-gel process. The structure of NPs was investigated using X-ray diffraction (XRD), scanning electron microscope (SEM), energy-dispersive X-ray (EDX), and differential reflectance spectroscopy (DRS). In addition, using statistical analyses, the effects of parameters such as the initial concentration of naphthalene, pH, contact time, and the optimal conditions on naphthalene removal were investigated.

Results: XRD patterns and SEM images of the samples confirmed the size of synthesized particles in nanometer. The EDX and DRS spectra analysis showed the presence of two elements (sulfur and nitrogen) and the optical photocatalytic activity in the visible region, respectively. The maximum level of naphthalene removal in the presence of sunlight was obtained to be about 93.55% using a concentration of 0.25 g of thiourea immobilized on glass microbullets at pH=5 and contact time of 90 minutes.

Conclusion: The rate of naphthalene removal using the immobilized TiO_2-N-S on glass microbullets was 93.55% in optimal conditions. Therefore, this method has an effective potential for naphthalene removal, and can be used to remove naphthalene from industrial wastewater.

Keywords: Sunlight, Aromatic hydrocarbons, Naphthalene, Glass microbullets, TiO_2-N-S nanoparticles

Received: 5 March 2020, Accepted: 2 August 2020, ePublished: 30 March 2021

Introduction

Water is a vital substance for human life and all people are aware of the importance of access to safe drinking water. One of the water pollutants is polycyclic aromatic hydrocarbons (PAHs). These compounds include a large group of organic compounds, with two or more aromatic rings that enter the environment through natural and industrial activities (1). Due to toxicity, mutagenicity, and carcinogenicity, these compounds have been ranked among the leading pollutants by the US Environmental Protection Agency (EPA), and the agency has declared a concentration of 0.5 mg/L of phenolic compounds in industrial effluent as permissible amount and even listed the lower concentrations of these compounds as permissible for aquatic and soil organisms (2).

Naphthalene ($C_{10}H_8$) is the first group of these hydrocarbons that has attracted the attention of many researchers in recent years as a common contaminant in water. Naphthalene is able to accumulate in water and soil for a long time (3). Exposure to naphthalene at high levels can cause hemolytic anemia, red blood cell breakdown (4), genetic mutations, fetal damage, congenital disorders, and kidney damage (5). Due to the extremely hazardous effects of naphthalene on human health, it is necessary to evaluate

© 2021 The Author(s); Published by Shahrekord University of Medical Sciences. This is an open-access article distributed under the terms of the Creative Commons Attribution License (http://creativecommons.org/licenses/by/4.0), which permits unrestricted use, distribution, and reproduction in any medium, provided the original work is properly cited.

www.SID.ir

Archive of SID

the likelihood of water pollution with this compound (6). Aerobic and anaerobic biological treatment, chemical oxidation, electrochemical oxidation, photochemical oxidation, coagulation, ion exchange filtration, adsorption onto activated carbon, buoyancy, biological degradation, and ozonation are important methods for the treatment of pollutants (7). Practically, there are limitations to the application of these methods, including the need for specific reactants, high cost, lack of removing small amounts of pollutants, production of by-products, and sludge production. Therefore, in recent decades, the use of new and more appropriate methods of wastewater treatment has been prioritized to maximize compliance with environmental regulations by researchers in this field. These methods also include those with chemical degradation, namely, advanced oxidation processes (AOPs) (8). AOPs include the effect of ultraviolet (UV) light on materials and the production of intermediates or active agents with oxidizing or reducing properties. The processes of AOPs themselves are subdivided into several large groups, the most important of which are photocatalytic oxidation processes.

Photocatalytic removal is carried out by UV radiation to the semiconductor surface such as ZnO or TiO_2, and oxidation is accomplished based on the activity of hydroxyl radicals, which are highly reactive species (9). As anatase crystals, inhomogeneous photocatalysts, including TiO_2, are the most popular photocatalysts due to their environmental friendliness, high optical activity, low cost, low toxicity, and high chemical and thermal stability (10). Over the past 30 years, TiO_2 nanoparticles (NPs) have been widely used as powders, but due to certain problems such as continuous mixing during work, high cost of filtration and centrifugation of powders for resuscitation, dispersion of NPs in solution and light blocking, efforts to stabilize photocatalysts on surfaces such as glass pellets, glass fibers (9,11), silica (12), activated carbon and zeolites and nanotubes are increasing. Optical degradation of pollutants as thin film fixation on a fixed bed has two major benefits, including the avoidance of high costs for catalyst separation (10,13,14) and lack of forming hazardous compounds due to advanced oxidation often used with other oxidants such as halogens (15). Besides, the broad TiO_2 gap has made it an efficient photocatalyst in the UV region. However, the sunlight naturally contains only 4% UV and the photocatalytic removal of naphthalene from aqueous solutions using UV increases the cost of purification and consumption, with practical limitations such as the low lifetime of the UV lamps and the consumption of electricity. UV lamps themselves are also considered a serious threat to the environment (10), so that methods such as doping with noble metals, metal ions and anions (C, N, S, F) are used to modify this inherent TiO_2 property and produce a new photocatalyst capable of retaining photocatalytic activity under visible sunlight (16,17). Muruganandham et al and Li et al doped the N and La on the TiO_2 lattice to reduce the energy gap and increase the TiO_2 optical activity in the visible light range (18, 19). In this study, titanium dioxide (TiO_2) was first synthesized using the sol-gel method, which is an ideal method for preparing homogeneous products with high purity in the production of metal oxides. Moreover, the absorption of TiO_2 was transferred to the range of light by doping nitrogen (N) and sulfur (S). Furthermore, with the stabilization of TiO_2-N-S on the bed of glass microbullets, the removal of naphthalene at concentrations of 5, 10, 15, 20, 25, and 40 ppm in the presence of sunlight was investigated considering the amount of total daily radiation and the optimal slope of pilot installation.

Materials and Methods

Photocatalyst synthesis

All chemicals were procured from Merck Co. (Germany), deionized (DI) distilled water from Zolal Company (Iran), and glass microbullets from Glass Seeds Company (Iran). In this study, TiO_2-N-S NPs were first synthesized by sol-gel method (20). TiO_2 sol was prepared by hydrolysis of tetrabutyl orthotitanate (TBOT) in acidic solution. For this purpose, the mixture was first mixed with 2.5 ml of TBOT, 10 mL ethanol, and 2.5 mL acetyl acetone. After 30 minutes, a clear yellow solution was obtained. Then, 2 mL of deionized water was added to the solution and the resulting solution was stirred for 10 minutes on the strainer. Concentrated hydrochloric acid and sodium hydroxide were used to adjust the pH of the cell at approximately 1.8. Next, 0.25 g of thiourea, as a source of nitrogen and sulfur, was added to the synthesized sol. The addition of thiourea results in the transfer of TiO_2 photocatalytic activity to the visible region. After 2 hours, a stable yellow sol was obtained. In order to stabilize the prepared sol, 40 g of glass microbullets with diameters of 450 to 600 microns were used in each round of synthesis. The glass microbullets were first rinsed with chloroform solution and then washed several times with deionized water and dried in an oven at 105°C for 1 hour. The glass microbullets were then coated in the sol solution using immersion for 10 minutes on a magnetic stirrer. They were then left in an oven at 60°C for 4 hours to evaporate ethanol. Finally, the fixed film on the bullets was calcinated in the furnace at 500°C for 1 hour and left in an ultrasonic bath for 15 minutes to eliminate possible contamination. One of the important properties of heterogeneous photocatalysts is the selection of the appropriate bed for the stabilization of TiO_2 NPs. The important considerations for selecting an appropriate bed include high surface area, strong bonding between the bed and the photocatalyst, the stability of the bed over a long period of time, no change in catalyst activity during and after removal of contamination, as well as stability during irradiation and acquiring resistance to certain radicals produced (21).

www.SID.ir

Archive of SID

Investigation of photocatalyst properties

The bonding gap of the samples was obtained using UV–visible spectroscopy (Avaspec 2048 Tech (AVANTES, USA) and according to the equation (1), where λ (nm) represents the wavelengths of adsorbed layers in the spectrum and Eg (eV) does the bonding gap.

$$E_g = \frac{1238.9}{\lambda} \quad (1)$$

Moreover, in the equation (2), S represents the average crystal dimension, k the crystal particle shape constant (0.89), θ the diffraction angle at the maximum peak, λ the x-ray wavelength, and β the peak width at half of its radius (22).

$$S = \frac{K\lambda}{\beta \cos\theta} \quad (2)$$

The surface morphology of the TiO_2 film was investigated by electron scanning microscope (SEM, Tescan MIRA3, Tescan Co., Czech Republic) equipped with X-ray diffraction (XRD) spectroscopy for elemental analysis.

Examination of photocatalytic optical activity

Optical degradation of naphthalene was investigated by synthesized photocatalyst under visible light and sunlight. The experiments were performed using 0.25 g of synthetic thiourea on 18 g of glass microbullets. The glass microbullets were distributed in four quartz glass tubes with a diameter and height of 8 and 200 mm, respectively, and placed on a flat mirror. Figure 1 illustrates the reactor used for photocatalytic experiments under sunlight. The volume of tested naphthalene solution in each test was adjusted at 500 mL and flow rate at 20 mL/min using a peristaltic pump in a closed system.

Photocatalytic experiments were carried out with initial concentrations of naphthalene 5, 10, 15, 20, 25, and 40 mg/L. The best naphthalene removal efficiency was obtained at pH 5. Residual concentrations of naphthalene were measured at a maximum amount of 276 λmax by a spectrophotometer (Perkin Elemer-Uv-Vis, USA), and naphthalene degradation efficiency was calculated using Equation 3. lambda

$$\text{Naphthalene removal}(\%) = \frac{C_0 - C_t}{C_0} \times 100 \quad (3)$$

where, C_0 represents the initial concentration and C_t the residual naphthalene concentration in solution.

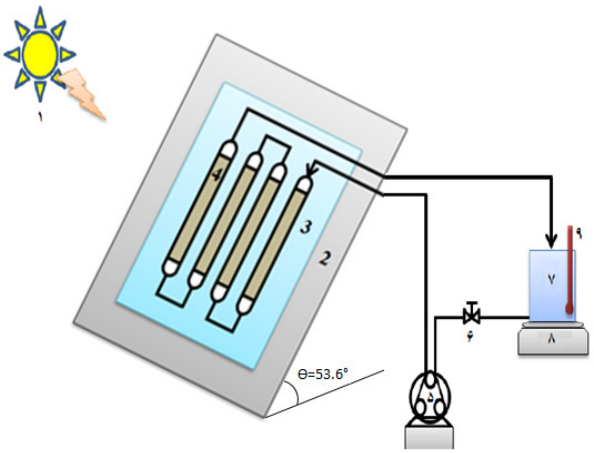

Figure 1. A schematic illustration of pilot used in the study: (1) sunlight; (2) wooden plate holder; (3) mirror; (4) photoreactors containing glass microbullets; (5) peristaltic pump; (6) flow valve and sampling; (7) tank containing naphthalene solution; (8) magnetic stirrer; and (9) alcohol thermometer.

Statistical analysis

To perform data analysis, SPSS version 18 (SPSS Inc., Chicago, IL) was used. The statistical significance of inter-group differences was investigated by one-way ANOVA and to determine which times are different from other times, the Dunnett's post hoc test was used. Finally, Tukey's test was used to compare experimental groups. The results were expressed by mean ± standard deviation and $P<0.05$ was considered as statistically significant.

Results

Synthesis, morphology, and structural properties of photocatalysts

The compound structure of the TiO_2-N-S NP phases prepared by XRD was determined. In order to investigate the formation of the anatase phase in the synthesized thin layers, the analysis was performed on the samples (23). The location of the peaks in the XRD of the anatase phase was measured according to the Joint Committee on Powder Diffraction Standards (JCPDS) of Card No. 0447-04 (23). Figure 2 illustrates the XRD of thin nanolayer of pure TiO_2 and thiourea-doped TiO_2. Peak 2θ=25.4° shows the main peak of the anatase phase (24), while the main peaks of Rutile and Brookite are 27.4° and 30.8°, in none of which the layers are seen (25). Therefore, all layers contain the anatase phase and no Rutile and Brookite phases. In Figure 2d, the anatase phase of the TiO_2-N-S powder sample was observed in peak 101 and 2θ=25.346°, and the particle size was calculated to be 14.5 nm.

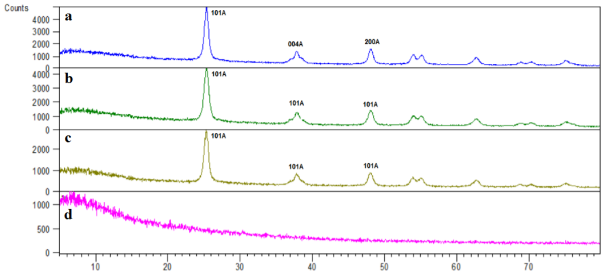

Figure 2. X-ray diffraction (XRD) spectrum from the surface of thin layer a: pure TiO_2 powder, b: TiO_2 coated on glass microbullets, c: TiO_2 doped with thiourea on glass microbullets, and d: uncoated glass microbullets

www.SID.ir

Archive of SID

In Figure 2c, the anatase phase of the TiO_2-N-S powder sample was observed at peak 101 and 2θ=25.348°, and the particle size was calculated to be 11.5 nm. The size of the NPs coated on the glass microbullets according to Figure 2b was calculated to be the same as the powder sample and 11.5 nm.

An example of an uncoated glass microbullet for comparison in the formation of phases is illustrated in Figure 2a, on which no peaks appear, resulting in NPs fixed on the bed of glass microbullets with an anatase phase structure that has photocatalytic properties. Figure 3 illustrates the SEM images obtained from NPs of TiO_2 thin layer and TiO_2-N-S coating on glass microbullets. The samples were examined in terms of appearance and morphology of the sample surface. Figures 3a and 3c illustrate that TiO_2 and TiO_2-N-S NPs are distributed as nanoblocks with a diameter of 15.58 and 11.8 nm, respectively, on a uniform surface. Figures 3b and 3d illustrate the thickness of TiO_2 thin layer and TiO_2-N-S coating on glass microbullets, respectively. Accordingly the thickness of the thin layer of pure TiO_2 and TiO_2-N-S is 809.93 and 693.68 nm, respectively.

Figure 4 illustrates the energy-dispersive X-ray (EDX) analysis of TiO_2 and TiO_2-N-S on glass microbullets. In this model, due to the presence of thiourea, the presence of two elements (sulfur and nitrogen) is observed in the mentioned film. The EDX analysis for the thin layer of coating TiO_2 with glass microbullets is illustrated in Figure 4a and the EDX analysis for TiO_2-N-S thin layer coated with glass microbullets is illustrated in Figure 4b. Elemental and atomic analysis of a thin layer of TiO_2 coated on glass microbullets was created by adding thiourea (CH_4N_2S) to the orthotitanate sol solution. Thus, the percentage of sulfur and nitrogen elements was obtained as 6.58% and 0.57% of the weight of studied samples, respectively.

The analysis of diffuse reflectance spectroscopy (DRS) nano-UV–vis diffuse reflectance spectra of pure TiO_2, TiO_2 doped with sulfur and nitrogen, and TiO_2-N-S doped with sulfur and nitrogen is illustrated in Figure 5. As can be seen, the diffusion coefficient value of the TiO_2-N-S spectrum in the visible region is stronger than pure TiO_2. To estimate the optical band gap energy of nanostructures, the Tauc plot (known as Kubelka–Munk model) was used (26). The absorption value obtained for the TiO_2 thin layer was 378 nm and for the TiO_2-N-S thin layer 416 nm, which was equivalent to the 2.3 eV energy gap of TiO_2 and 98.2 eV for TiO_2-N-S thin layer, respectively.

Removal of naphthalene with synthetic photocatalyst

The effect of pH on naphthalene degradation

The pH of the environment has different effects on the rate of oxidation reactions of materials. One of the most important determinants of removal efficiency is the

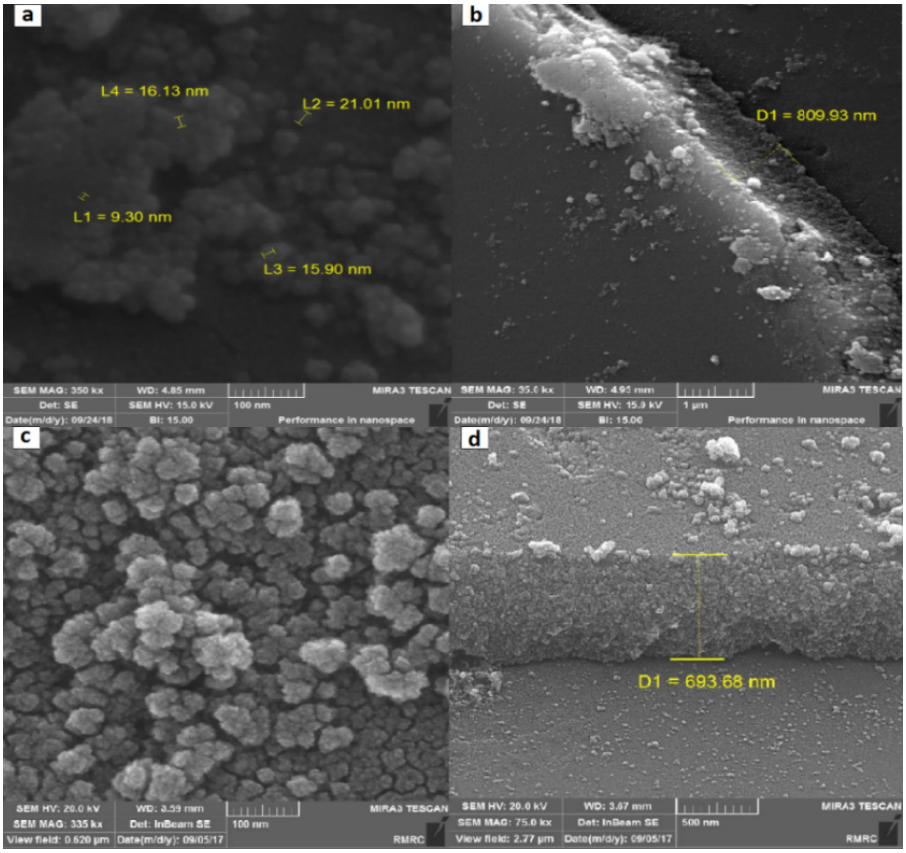

Figure 3. SEM images of nanometer size of pure TiO_2 particles (a) and thickness of pure TiO_2 coating layer (b) and nanometer size of TiO_2-N-S (c) coating particles and thickness of TiO_2-N-S (d) coating layer on glass microbullets.

www.SID.ir

Archive of SID

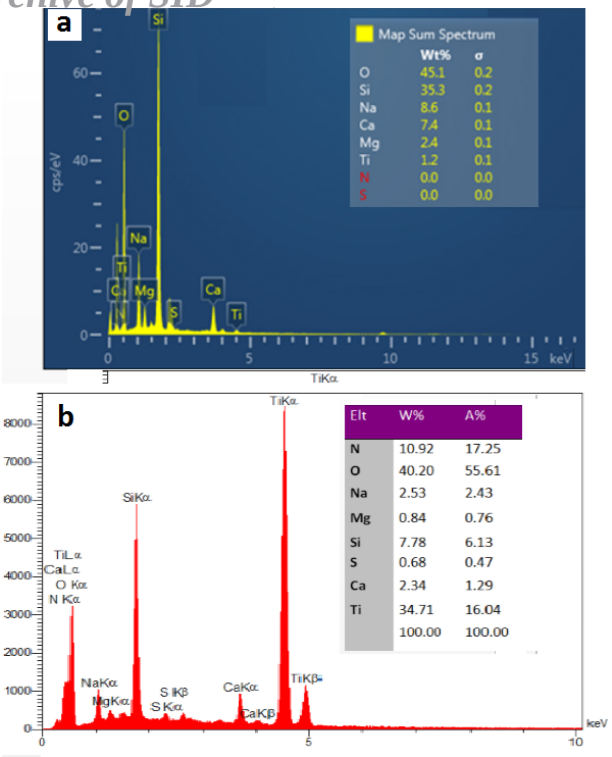

Figure 4. EDX analysis a: TiO_2 and b: TiO_2-N-S on glass microbullets.

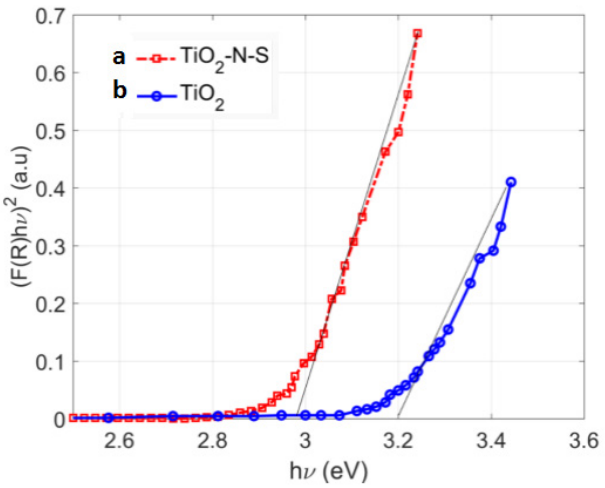

Figure 5. DRS analysis a: TiO_2 and b: TiO_2-N-S on glass microbullets.

electric charge level of the photocatalyst. The pH of the zero charge (pH_{pzc}) indicate the surface of catalyst has zero or neutral electric charge.(27). Figure 6 reports the zero point (PZC) pf the TiO_2 molecule at pH 6.25. Therefore, TiO_2 levels will have a positive charge in acidic state (a) and in weak alkaline conditions, (b), i.e. pH>6.25, the charge level of TiO_2 particles will be negative (18). Zhao et al reported that a positive charge on TiO_2 levels at pH less than 6 caused better migration of light-generated electrons and prevented the recombination of electrons and cavities, thus increasing the efficiency of the photocatalytic process (28). To determine the optimal pH, solutions with an initial constant concentration of 5 ppm of naphthalene

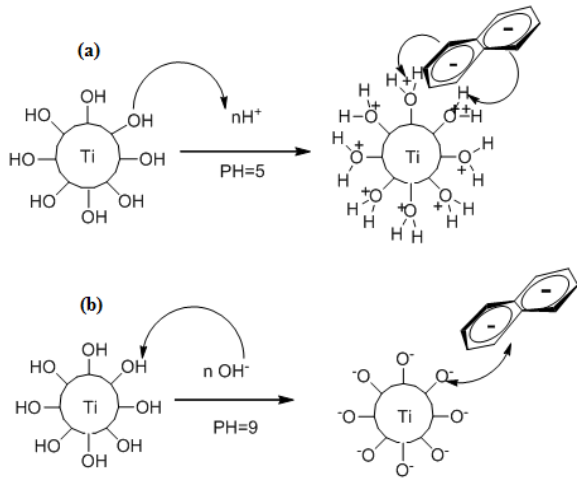

Figure 6. Point zero (pzc) of TiO_2 molecule at pH = 6.25; a) acidic pH, b) basic pH.

were first made at pHs 3, 5, 7, 9, and 10, and then the efficacy of naphthalene removal efficiency was investigated in the presence of TiO_2-N-S catalyst. Sampling was performed at intervals of 0, 30, 60, 90, 120, 150, 180, 210, and 240 minutes and according to the standard method at a wavelength of 276 nm. In addition, the amount of adsorption of samples was read with a spectrophotometer and the percentage of naphthalene removal using equation 3. According to the results shown in Table 1, the highest efficiency of naphthalene removal was obtained at pH 5 and 90 minutes, equivalent to 79.33±0.41, with a statistically significant difference with other pHs during this period ($P<0.05$).

Investigating the Effect of Naphthalene Initial Concentration

After determining the optimal pH, naphthalene solutions with concentrations of 5, 10, 15, 20, 25, and 40 ppm were prepared at a constant pH of 5 and tested at each concentration using a TiO_2-N-S photocatalyst under sunlight. Table 2 shows the naphthalene optical degradation with different initial concentrations in the presence of the TiO_2-N-S photocatalyst under sunlight. Accordingly, with increasing concentration and contact time, the removal efficiency of naphthalene increased and up to 90 minutes of contact time, this increasing trend was observed in all concentrations and no significant changes in naphthalene removal efficiency were observed since 90 minutes.

Investigating the Effect of Solar Radiation on the Optical Removal of Naphthalene

In order to investigate the effect of total light (total solar radiation, TSR) on naphthalene removal, information about total and instantaneous radiation of Shahrekord meteorological synoptic station, which was located at a distance of 3640.77 m from the pilot installation, was

www.SID.ir

Archive of SID

Table 1. Percentage of naphthalene optical degradation at constant concentration of 5 ppm and different pH groups in the presence of TiO_2-N-S photocatalyst under sunlight

pH	Time (min)							
	30	60	90	120	150	180	210	240
3	46.94±6.69	58.76±1.89*	68.36±5.39*	75.52±4.45	76.14±3.26	86.3±0.86	62.99±12.39	68.05±4.12
5	61.23±0.89	72.52±2.79	79.33±0.41**	75.78±3.77*	75.50±2.25	75.56±2.22	71.80±3.14	63.51±1.49
7	28.79±19.84*	42.26±8.66	54.66±3.78*	56.64±2.59	55.81±3.50*	59.02±1.53*	56.53±2.71	55.25±1.41
9	8.07±3.29	11.43±8.80	14.77±7.67	4.09±1.79	11.45±3.15	9.12±1.38	9.10±1.35	5.72±3.15
10	4.26±0.89	6.83±1.39	7.18±2.26	4.44±2/28	6.60±1.89	4.26±0.67	5.67±1.92	4.72±1.71

The data is based on the standard deviation of the average removal efficiency. * In five pH groups and in each time group, there is a significant statistical difference ($P<0.05$).
** There is a statistically significant difference between five pH groups and eight time groups ($P<0.05$).

Table 2. Percentage of naphthalene optical degradation at different initial concentrations in the presence of TiO_2-N-S photocatalyst under sunlight

Concentration (ppm)	Time (min)									
	10	25	30	60	90	120	150	180	210	240
Blank	0.12±0.01	0.72±0.03	2.2±0.1	4.5±0.2	5.56±0.15	6.4±0.36	6.3±0.31	7.58±0.53	8.63±0.47	9.56±0.50
5	37.26±0.74	40.26±3.05*	47.16±1.31	16.16±0.94	77.02±0.8	72.85±3.12	72.87±3.22	71.99±3.91	76.23±4.06*	81.10±1.87*
10	31.58±2.87	47.50±0.88**	49.86±1.88	63.57±1.05	72.25±0.7*	70.32±1.08	70.32±1.01	73.08±3.08	75.50±1.16*	66.16±1.88*
15	37.42±1.90	61.39±4.35	66.4±4.35*	79.94±3.1*	86.85±0.8	86.55±2.59	86.55±2.59*	83.5±2.59	83.63±2.38	85.54±2.09
20	33.09±1.46	57.51±4.01	60.92±1.90*	79.94±3.31*	76.53±2.31	77.87 ±3.52*	77.85±3.54	81.83±1.46	85.05±1.89	83.68±2.22
25	71.10±0.95*	78.74±1.60	82.94±1.52	85.30±1.81	88.27±0.93	86.26±1.66	86.26±1.66	83.85±0.11	86.47±1.32	85.79±0.49
40	66.47±3.23*	82.32 ±1.44**	81.97±3.55	85.32±1.83	93.52 ±0.53**	93.28±0.29*	93.38±0.22*	89.52±3.86*	91.99±2.25*	91.16±3.66*

The data is based on the standard deviation of the average deletion efficiency. Among the six concentration groups and 11 time groups, all groups had a statistically significant difference with control ($P<0.001$).
* There is a statistically significant difference between six concentration groups in each time group.
** There is a statistically significant difference between six concentration groups and 11 time groups ($P<0.05$).

examined. Due to the fact that the optimal conditions for removing naphthalene were obtained within 90 minutes, the total and instantaneous amount of radiation during 90 minutes of contact of naphthalene solution with the photocatalyst was extracted from the statistics of Shahrekord meteorological solar radiation (Table 3). Accordingly, the efficiency of naphthalene removal increased with increasing radiation. According to the isotropic model (29), the best slope of installing panels containing mirrors and glass tubes against sunlight in spring, summer, autumn, and winter is equal to 2.66°, 11.33°, 53.63°, and 48.33° angles. In general, the optimal annual installation angle is 29 degrees, which is almost close to the latitude of Shahrekord with a difference of less than 10% (30). In the study, the panel containing glass tubes was installed at an angle of 53.6 degrees to the horizon.

Intermediate compounds resulting from naphthalene decomposition

To evaluate the intermediate compounds obtained from the degradation process of naphthalene photolysis with TiO_2-N-S photocatalyst, gas chromatography-mass spectrometry (GC-MS) device was used with Agilent Technologies 7890 A gas chromatography technique and Agilent Technologies 5975C mass spectrometer (USA). Based on the inhibition time factor as well as the library evaluation of the instrument regarding mass spectrum interpretation, the intermediate compounds include phthalic acid, 2-formylcinnamaldehyde, 2- carboxy cinnamaldehyde, and ethanoic acid. The proposed mechanism for naphthalene removal is the oxidation process in the presence of OH and HO_2 radicals. It should be noted that previous studies have also suggested intermediate compounds resulting from the degradation of naphthalene photosynthesis and degradation mechanisms, which is in satisfactory agreement with the proposed results of this study (31,32). The results of GC-MS of the solution after irradiation at 120th minute indicate the removal of intermediates, and finally the mineralization of intermediate organic compounds and conversion to CO_2 gas and H_2O.

Discussion

In this study, the TiO_2-N-S photocatalyst was synthesized and fixed on glass microbullets using the sol-gel method to remove naphthalene from aqueous media. The morphological and structural characteristics of the photocatalyst using XRD, SEM, EDX, and DRS analyses showed that the photocatalyst was well fixed and synthesized on a fixed surface (glass microbullets). According to Figures 2c and 2b, the XRD analysis of the samples showed the anatase phase in the powder samples and the samples fixed on the glass microbullets bed, respectively, and the diameter of the NPs was obtained in both stabilized states on the surface of microbullets and NPs on very fine and homogeneous powder particles at 11.5 nm. Photocatalysts are used in the anatase phase under UV radiation and exhibit optical activity and catalytic properties (25).

According to the research by Zhuang et al, an increase

www.SID.ir

Archive of SID

Table 3. Effect of TSR on removal efficiency of naphthalene at different concentrations under the photocatalyst TiO_2-N-S

Naphthalene solution concentration (ppm)	pH Primary solution	Optimal removal efficiency %	pH The final solution	TSR momentary (w/ m^2)	TSR daily (w/ m^2)	Sunny hours (h)	%UV	Time sampling (h)
5	4.924	50.59	5.711	528.42	1469	9.2	4	14
5	4.925	60.43	5.765	722.95	2110	10.7	5	10.30
5	6.05	70.75	5.591	722.51	2265	10.4	6	14
10	5.027	71.44	5.218	739.39	2144	9.3	5.5	14
15	5.378	87.74	5.674	705.1	1612	9.1	6	11.40
20	4.985	77.92	5.312	522.17	1424	9.2	4	14
25	4.895	87.36	5.698	527.22	1437	9.8	4	14
40	4.922	93.24	5.303	579.22	1349	8.7	4	11.10

TSR, total solar radiation

in thiourea leads to a higher accumulation of nanometer particles in some areas (33), which is clearly seen in the SEM images of samples (Figures 3a and 3c). In general, nanometer-sized photocatalyst particles tend to accumulate due to the van der Waals force between the surface of the particles (34). According to the studies by Brindha et al and Sathish *et al* (34 , 35), the diameter of TiO_2-N-S NPs in the temperature range of 500°C was reported to be 15 nm, which is close to 14.1 nm of pure TiO_2 NPs. According to Figure 4b, EDX analysis, and elemental analysis of TiO_2-N-S, using thiourea in the catalyst structure leads to the weight percentage of sulfur and nitrogen elements as 6.85% and 0.57%, respectively. Moreover, in comparison with the case where thiourea is not used (Figure 4a), which uses only pure TiO_2, the presence of more titanium along with sulfur and nitrogen elements is observed. TiO_2 photocatalytic impurification with sulfur and nitrogen non-metals in accordance with the views of Zhuang et al and Hong et al has a significant effect on the removal of organic and mineral pollutants from aquatic environments (33, 36).

Comparing the DRS spectrum of pure TiO_2 (Figure 5a) and TiO_2 doped with sulfur and nitrogen (Figure 5b), the addition of two non-metallic elements of sulfur and nitrogen in the crystal structure of TiO_2 powder leads to a narrower energy gap and photocatalyst activity transfer of the TiO_2 to the visible area (37). According to researchers such as Zhang et al and Masoudipour et al, this energy gap is thinner than the mixture of P and non-metallic orbitals and 2P of TiO_2 oxygen (38,39). Shifu et al. used gas ammonia to dope nitrogen in a TiO_2 photocatalyst and stabilize it on the surface of hollow glass surfaces. They reported that the addition of nitrogen not only did not adversely affect the transfer of the TiO_2 phase from Rutile to anatase, but also caused the transfer of TiO_2 adsorption about 60 nm to the visible area (40). In the study, the absorption value of 38 nm was transferred to the visible area, which is in agreement with the results of Brindha et al and Rokhmat et al (34,41).

The results of this study showed that the rate of naphthalene removal is strongly dependent on the pH function and the contact time of the solution so that with decreasing pH, the efficiency of naphthalene removal increases. According to the results of Table 2, at a concentration of 5 ppm and the duration of 90 minutes of solution's contact with the photocatalyst, the removal efficiency increased from 7.28±2.69 at pH 10 to 79.31±0.41 at pH 5, indicating a statistically significant difference among five groups of pH and eight time groups with other pH and time groups ($P<0.05$). Avisar et al investigated the effect of solution pH on the simultaneous purification and elimination of polymorphic sulfamethoxazole (SMX), dextracycline (OTC), and ciprofloxacin (CIP) compounds in the presence of UV radiation. Their results showed that when these compounds were examined separately, increasing the pH of the solution from 5 to 7 led to a decrease in SMX degradation rate and an increase in OTC and CIP degradation rates, and when used as a mixture, the best result was obtained at pH 5, and the rate of SMX degradation reached 99% and the rate of OTC and CIP degradation increased from 54% and 26% in pH 7 to 91% and 96% in pH 5, respectively, which is consistent with the results of our study (42). Therefore, the pH of the solution plays a key role in the removal of aromatic compounds in aquatic environment. Moreover, as Table 3 shows, at the initial pH of 5 and approximately 5 of naphthalene solutions, the pH value increased for 90 minutes of contact with the photocatalyst and reached a maximum of 5.765, which according to Figure 6, the naphthalene load in this range is positive and better electron migration has taken place on the surface of the photocatalyst, and the destructive power of naphthalene is increasing (18).

The initial concentration of the solution was another important factor for the efficiency of naphthalene removal. According to Table 2, there was no significant statistical difference in all concentrations and the same time, so that at 10 minutes of contact, 25 and 40 ppm concentrations and at 20 minutes of contact time, concentrations of 15, 25, and 40 ppm, and at 30 and 60 minutes of contact

www.SID.ir

Archive of SID

time, concentrations of 15 and 20 ppm, and at 90 minutes of contact time, 10 and 40 ppm concentrations of naphthalene solution were statistically significant ($P<0.05$). Moreover, at 40 ppm naphthalene solution at contact times of 10, 20, 25, 90, 120, 150, 180, 210, and 240 minutes, there was a statistically significant difference in all concentrations ($P<0.05$), and during contact times of 30 and 60 minutes, there was no statistically significant difference with other concentrations ($P>0.05$).

Statistical results showed that increasing the concentration of naphthalene solution is very effective in the process of photocatalytic removal of TiO_2-N-S and the maximum efficiency of naphthalene removal was obtained in acidic conditions (pH=5) and at 40 ppm concentration of naphthalene solution at contact time of 90 minutes. Based on the results, the removal efficiency of naphthalene with TiO_2-N-S NPs increased with increasing contact time and decreasing pH. Although naphthalene removal increases over time up to 90 minutes, the removal power of the photocatalyst decreases with increasing contact time. After 90 minutes, the amount of removal changes is very small. Although naphthalene degradation is based on oxidation, naphthalene must first come to the surface of the microglia for oxidation to occur, but the reason for the decrease in naphthalene removal efficiency with increasing contact time can be considered in saturation of absorption points on the NP surface (43).

Karimi et al in a study of advanced oxidation removal of naphthalene by H_2O_2/UV/TiO_2 process from aqueous media found that due to the use of 20 ppm H_2O_2 at pH 3 and the radiation intensity of 5.6 (w/cm^2) at 254 nm wavelength, conditions for mineralization of naphthalene at a concentration of 15 ppm are provided after 100 minutes of contact time and the removal efficiency is reported to be 73% (44), while in the current study, the removal efficiency of naphthalene at the same concentration after 64.6 minutes of contact with photocatalyst reached 73%, which represents the high power of this photocatalyst in removing naphthalene without using disposable UV lamps and H_2O_2 oxidizing compound. During a constant period, with increasing the concentration of the solution, the efficiency of naphthalene removal increases. Moreover, in case of the increase of the solution concentration from 5 to 40 ppm and the contact time of 90 minutes, the removal efficiency increased from 72.5% to 93.26%, respectively. This is due to the increased power of the concentration gradient with higher concentrations of naphthalene. At lower concentrations, the ratio of the initial number of naphthalene moles to the available adsorption sites is low, and as a result some of the initial adsorption will be independent of the initial concentration (45).

Muthukumar et al coated the Fe-ZnO NPs on the *Amaranthus dubius* plant and synthesized the catalyst (Fe-ZnO-NP) and used it under UV radiation to remove naphthalene. Optimal conditions for naphthalene removal were reported at initial concentration of 40 ppm and pH 4, using 60 mg/L Fe-ZnO-NP as being 92.33% at 240 minutes in exposure to a 16-watt UV lamp (46). However, the results of current study showed that the naphthalene solution at 40 ppm exhibited a higher removal efficiency at a lower contact time (90 min) and exposure of TiO_2-N-S photocatalyst to sunlight.

Masoudipour et al used TiO_2-N-S NPs stabilized on glass microbullets to remove cyanide from the aqueous medium in the presence of sunlight and reported removal efficiency of cyanide solution at optimal concentrations of 50 ppm, pH 11 and 240 minutes as being 100% (47). However, in our study, the optimal conditions for naphthalene removal occur in a shorter time and at a pH close to neutral pH, which is cost-effective in terms of time and energy. Moreover, the amount of sunlight has a positive effect on the removal of naphthalene.

According to the results of Table 3, in the initial constant concentration of 5 ppm of naphthalene solution and radiations of 528.42, 722.95, and 772.51 w/m^2, the efficiency of naphthalene removal is equal to 50.59, 60.43, and 70.75, respectively. This shows that increasing the amount of irradiation increases the removal of naphthalene, and in close ranges of the amount of radiation and different concentrations of naphthalene, the concentration factor plays a decisive role in the efficiency of naphthalene removal (45), so that the efficiency of naphthalene removal in concentration of 20 ppm and the amount of radiation 522.17 w/m^2 was equal to 77.92% and in the concentration of 25 ppm and the amount of radiation 527.22 w/m^2 was equal to 78.36%; however, the amounts of radiation were not substantially different. As a result, the efficiency of naphthalene removal at higher concentrations increased, which is related to the number and amount of surface sites present at higher concentrations in naphthalene solution (21).

Xiaolong et al studied the highly efficient destruction of PAHs by Ag_3PO_4-doped graphene oxide under sunlight, and 7 minutes following exposure of the solution to the photocatalyst, the intermediate compounds 1-naphthol and 1,4-dinaphthol and 1,4-naphthoquinone and 1,2-benzenedicarboxylic acid and dialkyl ester and after 20 minutes of contact, two compounds 1,4-dinaphthol and 1,4-naphthoquinone were identified with GC-MS, which eventually converted to dialkyl ester and 1,2-benzenedicarboxylic acid (48). However, in the current study, the intermediate compounds obtained from naphthalene oxidation under sunlight were converted to water and carbon dioxide using the TiO_2-N-S photocatalyst.

Conclusion

In this study, synthesis and stabilization of thin layer of TiO_2-N-S by sol-gel method on a fixed bed (glass microbullets) was successfully performed. The composition

www.SID.ir

Archive of SID

of the thin layer along with its morphological and structural characteristics showed that the optical activity of the photocatalyst was directed towards visible light and could be used under the pure and endless energy of the sun to remove polyaromatic and resistant compounds and decompose them into harmless products such as water and carbon dioxide.

Conflict of Interests

None to be declared.

Ethical Approval

This study was approved by Islamic Azad University, Tehran Science and Research Branch and the ethics code of the dissertation (95/981) was made on 20/09/2016.
(Approval letter by Islamic Azad University NO. P/215 dated 08/07/2020).

Acknowledgments

The authors would like to thank the Head and Personnel of the Water and Wastewater Company of Chaharmahal and Bakhtiari Province (Iran) for their support and assistance during this research project.

References

1. Chen Y, Sun C, Zhang J, Zhang F. Assessing 16 Polycyclic Aromatic Hydrocarbons (PAHs) in River Basin Water and Sediment Regarding Spatial-Temporal Distribution, Partitioning, and Ecological Risks. Pol J Environ Stud. 2018;27(2):579-89. doi: 10.15244/pjoes/75827.
2. Hussain K, Balachandran S, Hoque RR. Sources of polycyclic aromatic hydrocarbons in sediments of the Bharalu River, a tributary of the River Brahmaputra in Guwahati, India. Ecotoxicol Environ Saf. 2015;122:61-7. doi: 10.1016/j.ecoenv.2015.07.008.
3. Li P, Diao X, Zhang Y, Xie Y, Yang F, Zhou H, et al. Polycyclic aromatic hydrocarbons in surface sediment from Yangpu Bay, China: distribution, sources and risk assessment. Mar Pollut Bull. 2015;99(1-2):312-9. doi: 10.1016/j.marpolbul.2015.07.039.
4. Still K, Jederberg W, Luttrell W. Derivation of occupational exposure limits. In: Toxicology Principles for the Industrial Hygienist. Fairfax, VA: American Industrial Hygiene Association (AIHA); 2008. p. 347.
5. Liu C, Zhang L, Liu R, Gao Z, Yang X, Tu Z, et al. Hydrothermal synthesis of N-doped TiO_2 nanowires and N-doped graphene heterostructures with enhanced photocatalytic properties. J Alloys Compd. 2016;656:24-32. doi: 10.1016/j.jallcom.2015.09.211.
6. Bojes HK, Pope PG. Characterization of EPA's 16 priority pollutant polycyclic aromatic hydrocarbons (PAHs) in tank bottom solids and associated contaminated soils at oil exploration and production sites in Texas. Regul Toxicol Pharmacol. 2007;47(3):288-95. doi: 10.1016/j.yrtph.2006.11.007.
7. Yonar T. Decolorisation of textile dyeing effluents using advanced oxidation processes. In: Advances in Treating Textile Effluent. Rijeka: IntechOpen; 2011. p. 1-26. doi: 10.5772/18908.
8. Daneshvar N, Salari D, Khataee AR. Photocatalytic degradation of azo dye acid red 14 in water: investigation of the effect of operational parameters. J Photochem Photobiol A Chem. 2003;157(1):111-6. doi: 10.1016/s1010-6030(03)00015-7.
9. Laera G, Jin B, Zhu H, Lopez A. Photocatalytic activity of TiO_2 nanofibers in simulated and real municipal effluents. Catal Today. 2011;161(1):147-52. doi: 10.1016/j.cattod.2010.10.037.
10. Zangeneh H, Zinatizadeh AAL, Habibi M, Akia M, Isa MH. Photocatalytic oxidation of organic dyes and pollutants in wastewater using different modified titanium dioxides: a comparative review. J Ind Eng Chem. 2015;26:1-36. doi: 10.1016/j.jiec.2014.10.043.
11. Li H, Zhang W, Zou L, Pan L, Sun Z. Synthesis of TiO_2–graphene composites via visible-light photocatalytic reduction of graphene oxide. J Mate Res. 2011;26(8):970-3. doi: 10.1557/jmr.2011.22.
12. Hosseinzadeh Sani M, Khosroabadi S, Shokouhmand A. A novel design for 2-bit optical analog to digital (A/D) converter based on nonlinear ring resonators in the photonic crystal structure. Opt Commun. 2020;458:124760. doi: 10.1016/j.optcom.2019.124760.
13. Kalantari M, Karimkhani A, Saghaei H. Ultra-wide mid-IR supercontinuum generation in As2S3 photonic crystal fiber by rods filling technique. Optik. 2018;158:142-51. doi: 10.1016/j.ijleo.2017.12.014.
14. Saghaei H. Supercontinuum source for dense wavelength division multiplexing in square photonic crystal fiber via fluidic infiltration approach. Radioengineering. 2017;26(1):16-22. doi: 10.13164/re.2017.0016.
15. Bozzi A, Guasaquillo I, Kiwi J. Accelerated removal of cyanides from industrial effluents by supported TiO_2 photocatalysts. Appl Catal B Environ. 2004;51(3):203-11. doi: 10.1016/j.apcatb.2004.02.014.
16. Fan J, Zhao Z, Liu W, Xue Y, Yin S. Solvothermal synthesis of different phase N- TiO_2 and their kinetics, isotherm and thermodynamic studies on the adsorption of methyl orange. J Colloid Interface Sci. 2016;470:229-36. doi: 10.1016/j.jcis.2016.02.045.
17. Fagan R, McCormack DE, Hinder S, Pillai SC. Improved high temperature stability of anatase TiO_2 photocatalysts by N, F, P co-doping. Mater Des. 2016;96:44-53. doi: 10.1016/j.matdes.2016.01.142.
18. Muruganandham M, Swaminathan M. Advanced oxidative decolourisation of Reactive Yellow 14 azo dye by UV/TiO2, UV/H2O2, UV/H2O2/Fe2+ processes—a comparative study. Sep Purif Technol. 2006;48(3):297-303. doi: 10.1016/j.seppur.2005.07.036.
19. Li H, Wang J, Li H, Yin S, Sato T. Photocatalytic activity of (sulfur, nitrogen)-codoped mesoporous TiO_2 thin films. Res Chem Intermed. 2010;36(1):27-37. doi: 10.1007/s11164-010-0111-z.
20. Saghaei H. Dispersion-engineered microstructured optical fiber for mid-infrared supercontinuum generation. Appl Opt. 2018;57(20):5591-8. doi: 10.1364/ao.57.005591.
21. Yang J, Bai H, Jiang Q, Lian J. Visible-light photocatalysis in nitrogen–carbon-doped TiO_2 films obtained by heating TiO2 gel–film in an ionized N2 gas. Thin Solid Films. 2008;516(8):1736-42. doi: 10.1016/j.tsf.2007.05.034.
22. Farrokhi M, Yang JK, Lee SM, Shirzad-Siboni M. Effect of organic matter on cyanide removal by illuminated titanium dioxide or zinc oxide nanoparticles. J Environ Health Sci Eng. 2013;11(1):23. doi: 10.1186/2052-336x-11-23.
23. Mohammadi-Moghadam F, Sadeghi M, Masoudipour N. Degradation of cyanide using stabilized S, N-TiO_2 nanoparticles by visible and sun light. J Adv Oxid Technol. 2018;21(1). doi: 10.26802/jaots.2017.0101.
24. Bourikas K, Kordulis C, Lycourghiotis A. Titanium dioxide (anatase and rutile): surface chemistry, liquid-solid interface chemistry, and scientific synthesis of supported catalysts.

www.SID.ir

Archive of SID

Chem Rev. 2014;114(19):9754-823. doi: 10.1021/cr300230q.
25. Akbarzadeh R, Umbarkar SB, Sonawane RS, Takle S, Dongare MK. Vanadia–titania thin films for photocatalytic degradation of formaldehyde in sunlight. Appl Catal A Gen. 2010;374(1-2):103-9. doi: 10.1016/j.apcata.2009.11.035.
26. Jafari A, Sadeghi M, Tirgir F, Borghaei SM. Sulfur and nitrogen doped-titanium dioxide coated on glass microspheres as a high performance catalyst for removal of naphthalene (C10H8) from aqueous environments using photo oxidation in the presence of visible and sunlight. Desalin Water Treat. 2020;192:195-212. doi: 10.5004/dwt.2020.25659.
27. Njoku VO, Foo KY, Asif M, Hameed BH. Preparation of activated carbons from rambutan (*Nephelium lappaceum*) peel by microwave-induced KOH activation for acid yellow 17 dye adsorption. Chem Eng J. 2014;250:198-204. doi: 10.1016/j.cej.2014.03.115.
28. Zhao H, Xu S, Zhong J, Bao X. Kinetic study on the photo-catalytic degradation of pyridine in TiO_2 suspension systems. Catal Today. 2004;93-95:857-61. doi: 10.1016/j.cattod.2004.06.086.
29. Maleki A, Rahimi R, Besharti Sh. Determining the optimal angle of solar panels for flat panels for solar dryers in Shahrekord region. 8th National Congress of Agricultural Machinery Engineering (Biosystem) and Mechanization of Iran; Mashhad; 2013.
30. Liu BY, Jordan RC. The long-term average performance of flat-plate solar-energy collectors: with design data for the U.S., its outlying possessions and Canada. Sol Energy. 1963;7(2):53-74. doi: 10.1016/0038-092x(63)90006-9.
31. García-Martínez MJ, Canoira L, Blázquez G, Da Riva I, Alcántara R, Llamas JF. Continuous photodegradation of naphthalene in water catalyzed by TiO_2 supported on glass Raschig rings. Chem Eng J. 2005;110(1-3):123-8. doi: 10.1016/j.cej.2005.03.020.
32. Hykrdová L, Jirkovský J, Mailhot G, Bolte M. Fe(III) photoinduced and Q-TiO_2 photocatalysed degradation of naphthalene: comparison of kinetics and proposal of mechanism. J Photochem Photobiol A Chem. 2002;151(1-3):181-93. doi: 10.1016/s1010-6030(02)00014-x.
33. Zhuang J, Dai W, Tian Q, Li Z, Xie L, Wang J, et al. Photocatalytic degradation of RhB over TiO_2 bilayer films: effect of defects and their location. Langmuir. 2010;26(12):9686-94. doi: 10.1021/la100302m.
34. Brindha A, Sivakumar T. Visible active N, S co-doped TiO_2/graphene photocatalysts for the degradation of hazardous dyes. J Photochem Photobiol A Chem. 2017;340:146-56. doi: 10.1016/j.jphotochem.2017.03.010.
35. Sathish M, Viswanath RP, Gopinath CS. N, S-co-doped TiO_2 nanophotocatalyst: synthesis, electronic structure and photocatalysis. J Nanosci Nanotechnol. 2009;9(1):423-32. doi: 10.1166/jnn.2009.j095.
36. Hong S, Han Y, Zhang K, Wang M, Cui N, Du X, et al. TiO_2 nanosheet-redox graphene oxide/sulphur cathode for high-performance lithium-sulphur batteries. J Nanosci Nanotechnol. 2020;20(3):1715-22. doi: 10.1166/jnn.2020.16957.
37. Saghaei H, Van V. Broadband mid-infrared supercontinuum generation in dispersion-engineered silicon-on-insulator waveguide. J Opt Soc Am B. 2019;36(2):A193-A202. doi: 10.1364/josab.36.00a193.
38. Zhang J, Xu LJ, Zhu ZQ, Liu QJ. Synthesis and properties of (Yb, N)-TiO_2 photocatalyst for degradation of methylene blue (MB) under visible light irradiation. Mater Res Bull. 2015;70:358-64. doi: 10.1016/j.materresbull.2015.04.060.
39. Masoudipour N, Sadeghi M, Mohammadi-Moghadam F. Photo-catalytic inactivation of *E. coli* using stabilized Ag/S, N-TiO_2 nanoparticles by fixed bed photo-reactor under visible light and sunlight. Desalin Water Treat. 2018;110:109-16. doi: 10.5004/dwt.2018.22224.
40. Shifu C, Xuqiang L, Yunzhang L, Gengyu C. The preparation of nitrogen-doped TiO_2–xNx photocatalyst coated on hollow glass microbeads. Appl Surf Sci. 2007;253(6):3077-82. doi: 10.1016/j.apsusc.2006.06.058.
41. Sutisna, Rokhmat M, Wibowo E, Khairurrijal, Abdullah M. Prototype of a flat-panel photoreactor using TiO_2 nanoparticles coated on transparent granules for the degradation of Methylene Blue under solar illumination. Sustain Environ Res. 2017;27(4):172-80. doi: 10.1016/j.serj.2017.04.002.
42. Avisar D, Lester Y, Mamane H. pH induced polychromatic UV treatment for the removal of a mixture of SMX, OTC and CIP from water. J Hazard Mater. 2010;175(1-3):1068-74. doi: 10.1016/j.jhazmat.2009.10.122.

www.SID.ir